COMPARISON BETWEEN OPTICAL AND COMPUTER VISION ESTIMATES OF VISIBILITY IN DAYTIME FOG

Tarel, J.-P., Brémond, R., Dumont, E., Joulan, K.
Université Paris-Est, COSYS, LEPSIS, IFSTTAR, 77447 Marne-la-Vallée, FRANCE
jean-philippe.tarel@ifsttar.fr

Abstract

This paper investigates visibility in daytime fog as estimated optically with a visibility sensor and computationally with an image sensor. We use a database collected on a weather observation site equipped with both a forward scatter visibility meter and a CCTV camera. We implement a computer vision method based on the contrast sensitivity function of the human visual system to estimate the visibility level (VL) of targets located at different distances in the scene, and we study the relationship of the results with the extinction coefficient of the atmosphere, derived from the meteorological optical range (MOR) provided by the optical sensor. We show that Koschmieder's law, which predicts exponential reduction of visibility as a function of optical depth, applies not only to dark objects against the sky, but to other types of contrast as well.

Keywords: Fog, Meteorological Optical Range, Contrast, Visibility, Imaging, Computer Vision

1 Introduction

Fog is a quite common meteorological phenomenon. It happens in certain wind, temperature, and humidity conditions when vapour condenses into microscopic water droplets around airborne particles, causing the optical density of the atmosphere to rise dramatically. The net result is that visibility drops to levels where traffic becomes hazardous, with disrupting effects on ground (and other modes of) transport. Presently, the main solution to prevent such disruptions is to give warning to the drivers ahead of a foggy area, so that they can adapt their behaviour (Al-Ghamdi, 2007).

Fog detection and warning systems need to monitor the atmospheric visibility in order to trigger relevant advisory or compulsory messages. This is usually done by means of optical visibility sensors which directly or indirectly estimate the extinction coefficient k (expressed in m^{-1}), a measure of the light scattering power of the atmosphere in the Beer-Lambert law. The extinction coefficient is usually converted into the Meteorological Optical Range (MOR, expressed in m), which is more informative since it approximates the so-called meteorological visibility, i.e. the greatest distance at which a black object of suitable dimensions can be recognized by day against the horizon sky (CIE, 1987).

However, there's more to visibility than the contrast of a black object against the sky, especially when driving a motor vehicle in dense fog. Most objects of interest for the driver (markings, signs, other road users, obstacles, etc.) lie in the vicinity of the road; they are not always dark, nor uniformly coloured; and most of the time their background is not the sky, but some adjacent or distant surface. For such objects, exponential reduction of visibility with optical depth does not follow from Koschmieder's law in as straightforward a way as for a black object against the sky:

$$C = C_0 \exp(-kd) \tag{1}$$

where C is the contrast of the target at distance d, and C_0 is the contrast at very close range.

In this paper, we investigate the reduction of target visibility as a function of MOR in daytime fog. We worked with a database of images and MOR measurements. We implemented a computer vision algorithm to extract the visibility level of targets with different types of contrast at different distances. We studied the relationship between target visibility and extinction coefficient to verify the applicability of Koschmieder's law.

2 Description of the data

For this study, we used the Matilda database, which was collected on a weather observation site in Trappes, France, with the help of the French Meteorology Institute (Météo-France), in order to develop a camera-based method to estimate MOR (Hautière et al., 2011). The database contains images of a static outdoor scene grabbed every ten minutes 24/7 during a three day period which saw particularly diverse visibility and sky conditions. Each image is associated with a MOR value measured with a meteorological instrument on the same site.

The camera was an inexpensive one typically used in CCTV systems for traffic surveillance. It came with a 1/3" CCD black & white sensor with PAL definition. It was equipped with a 4-mm auto-iris lens which provided a horizontal field of view of about 64°. The images were captured by a digital video recorder in VGA definition and saved into JPG format. Samples are presented in Figure 1.

Figure 1 – Images from the Matilda database, grabbed in different visibility (top) and sky (bottom) conditions.

A depth map of the scene was built by projecting a digital terrain model provided by the French Geographic Institute (IGN) after calibrating the camera. The result is shown in Figure 2. As the model only contained the terrain and the buildings, we had to use a digital map to roughly estimate the position of other elements (equipment, vegetation) relative to the camera.

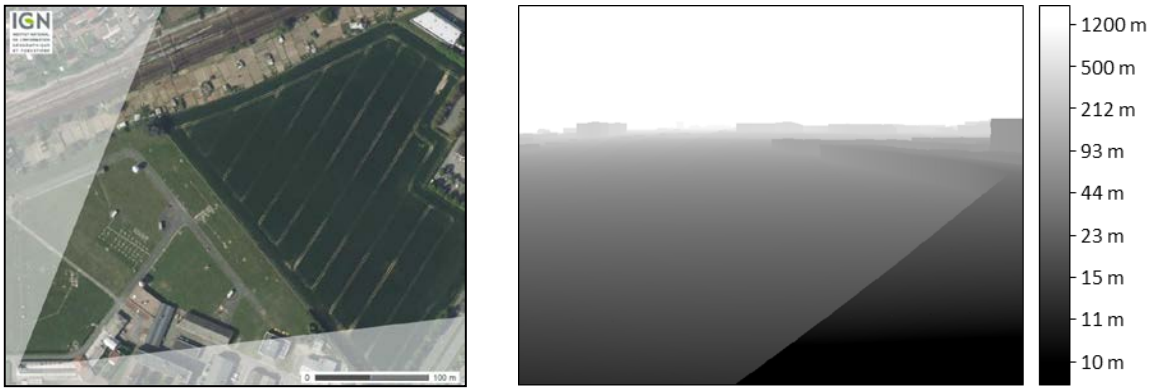

Figure 2 – Aerial image of the observation site (left) showing the field of view of the camera, and depth map of the scene (right).

Due to the optical characteristics of the camera, the spatial frequencies in the images approximately range between 0,02 and 5 cycles per degree, covering the lower half of the frequency domain detectable by the human visual system (Barten, 1999). The linear photometric response of the CCD sensor allows us to assume that the luminance in the scene is a linear function of the pixel values in the images. As we are investigating daytime visibility (photopic vision), we further assume that the adaptation luminance is high enough not to impact the visibility of contrasts (Weber's law), so that we do not need absolute luminance values to implement visibility models. Therefore, we simply use pixel intensity as a substitute for luminance.

3 Description of the method

We selected a number (21) of elements at different distances in the scene in order to investigate their visibility as a function of the extinction coefficient k, which is related to the MOR V_{met} by the approximate equation $V_{\text{met}} \approx 3 / k$ (WMO, 2012). We considered 4 types of "targets":

- Type 1: contrast of an object against the sky (e.g. the water towers, the trees);
- Type 2: contrast of an object against other objects in the background (e.g. the radar in front of the trees);
- Type 3: contrast between nearby but differently coloured horizontal or vertical surfaces (e.g. windows on a façade);
- Type 4: texture contrast (e.g., the lawn).

The distance of the targets was extracted from the depth map using the masks presented in Figure 3, and set to the minimum value when the target involved objects or surfaces at different distances. The distance from the camera to the closest target is 13 m, and that to the furthest is 1720 m; the sky is attributed an infinite distance. The distance and type of all targets are given in Table 1.

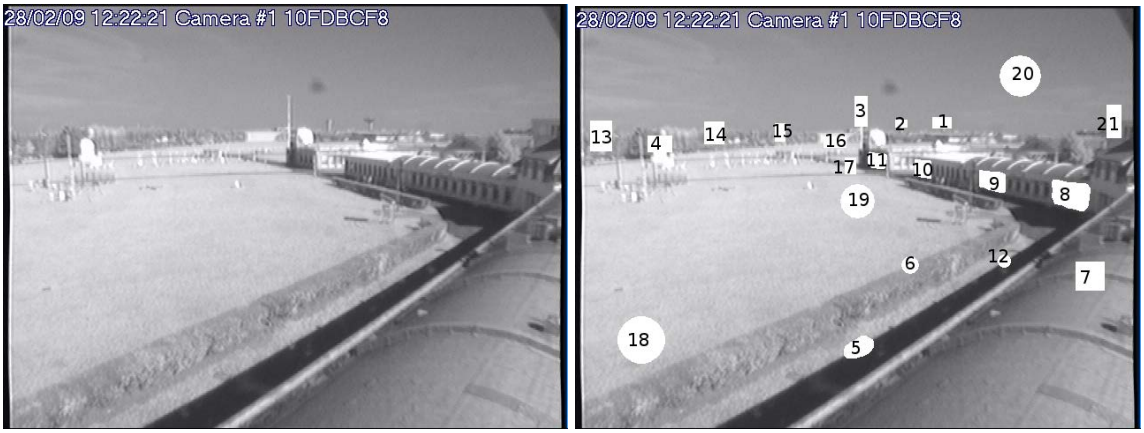

Figure 3 – Selection of elements at different distances in the scene where target visibility was estimated as a function of meteorological visibility.

Table 1 – Description of the targets

Target #	21	3	13	14	15	1	2	6	4	16	7	5	12	8	9	10	11	17	18	19	20
Distance (m)	100	146	230	350	500	1450	1720	28	202	470	13	18	35	60	73	94	110	120	20	70	∞
Type of contrast	1							2			3								4		

To assess the visibility of the selected targets, we set out to evaluate their Visibility Level (VL) as recommended by the CIE (1992). The VL characterizes the visibility of an object against its background. It is defined as the ratio of the actual contrast to the threshold contrast. The

threshold contrast is usually obtained by means of an empirical threshold-versus-intensity model such as Adrian's (1989). However, implementing such a model in real-world, spatially complex scenes, is often challenging, due to the difficulty of assigning a luminance value to the object or the background when neither is homogeneous (Colomb et al., 2006; Hautière et al., 2007; Brémond et al., 2013). Therefore, we chose to implement a more recent image processing approach which computes a VL map from the luminance map of the considered scene, based on the contrast sensitivity function (CSF) of the human visual system (Joulan et al., 2011a, 2011b). An example of VL map is presented in Figure 4. Target visibility (TV) values were then set for all targets to the maximum value inside their masks in the VL map. The results are presented in Figure 5 for a sample of each type of target.

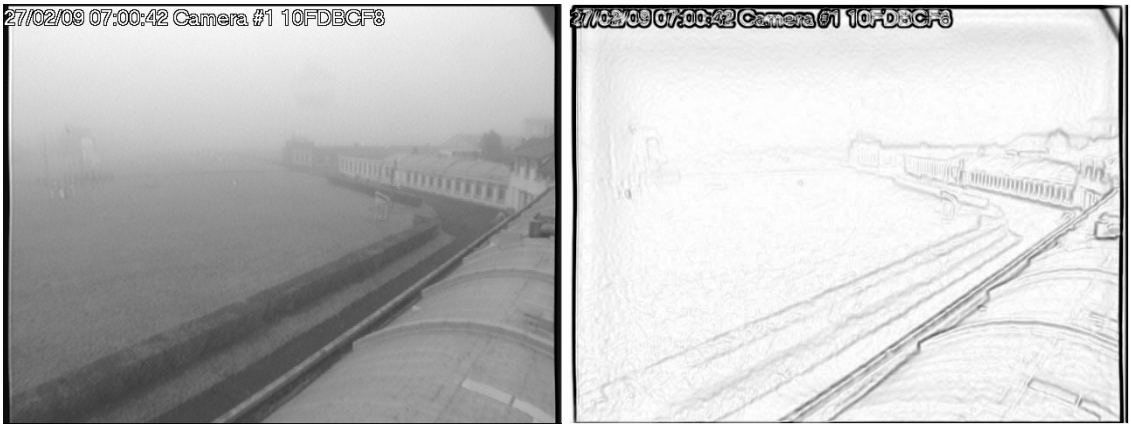

Figure 4 – Foggy scene image (left) and corresponding VL map (right), with higher VL values (up to 50) linearly mapped to lower grey levels.

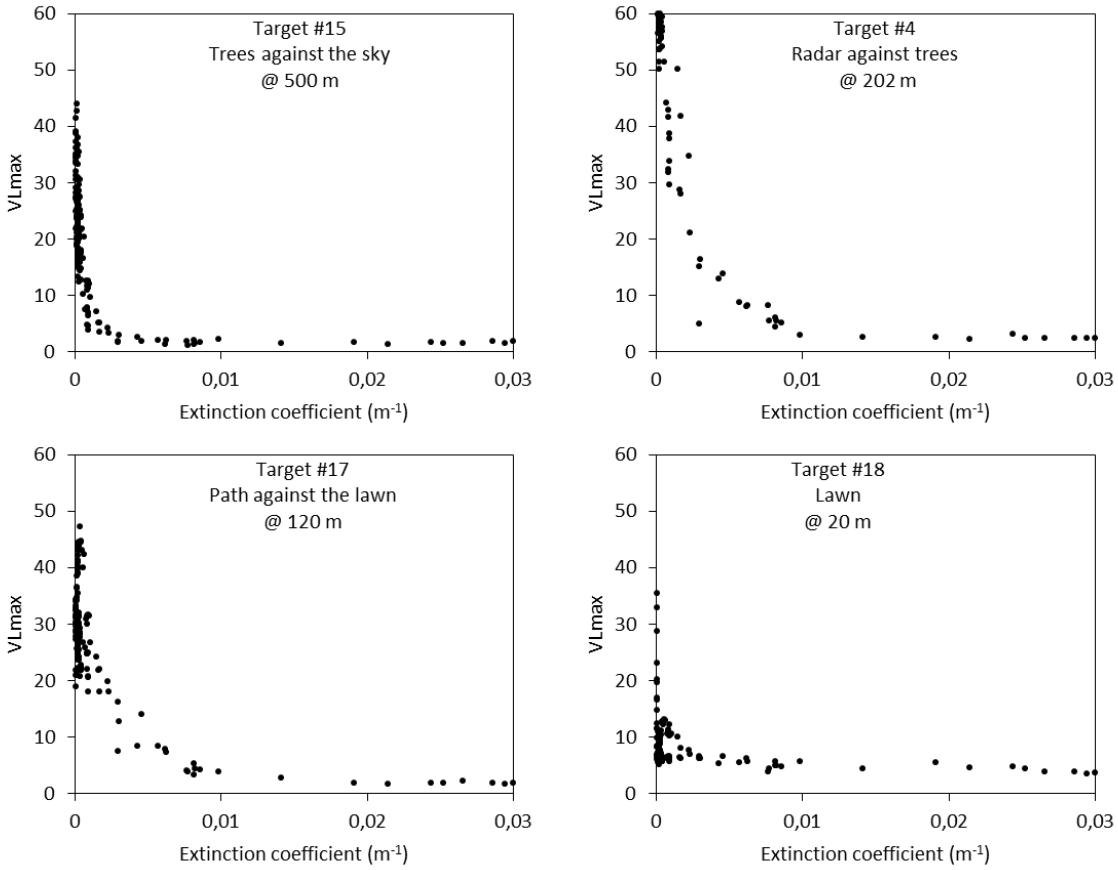

Figure 5 – Target visibility as a function of extinction coefficient ($k = 3 / V_{met}$) for different types of targets at different distances.

4 Analysis of the results

The first thing that we noted was the dispersion of TV values at lower values of the extinction coefficient, i.e. in good visibility conditions. This was expected, because in such conditions, contrast is much more dependent on daylight (depending on the position of the sun and the cloud cover) than in foggy conditions when lighting is diffuse. Therefore, we chose to focus on foggy conditions only, discarding data with MOR higher than 6 km (i.e., $k < 5.10^{-4}$ m^{-1}).

Our second observation was that the asymptote of TV as fog grows denser was close but not quite equal to zero. This can be explained by the presence of a certain level of noise in the images, due to the sensor and the JPG compression. In order to assess this level of noise, we selected an image grabbed in overcast sky conditions, and we looked at VL values in the sky region (dashed contour in Figure 6), where we expect no visible features. The resulting histogram (Figure 6) showed that image noise presented VL values up to 2,5. Therefore, we chose to discard data with TV below that threshold from our analysis.

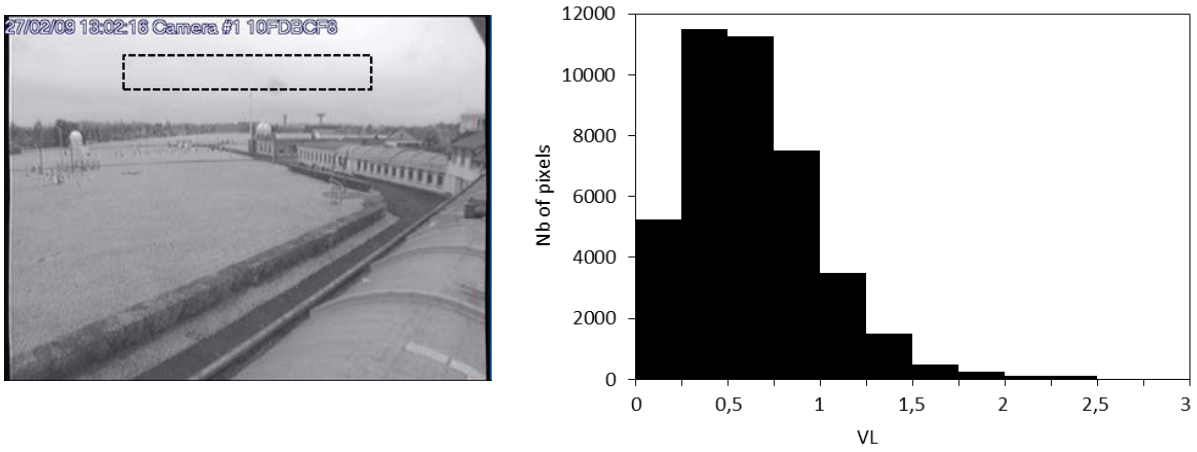

Figure 6 – Histogram of the visibility level in the sky region (clipped by the dashed line).

We wanted to test the hypothesis that TV follows an exponential function of extinction coefficient. Therefore, we performed simple linear regression analyses between the natural logarithm of TV and the extinction coefficient for each target. The results, illustrated with target #17 in Figure 7, broadly confirm the hypothesis. Furthermore, we found the slope of the linear fit to correspond approximately with target distance, as can be observed in Figure 8.

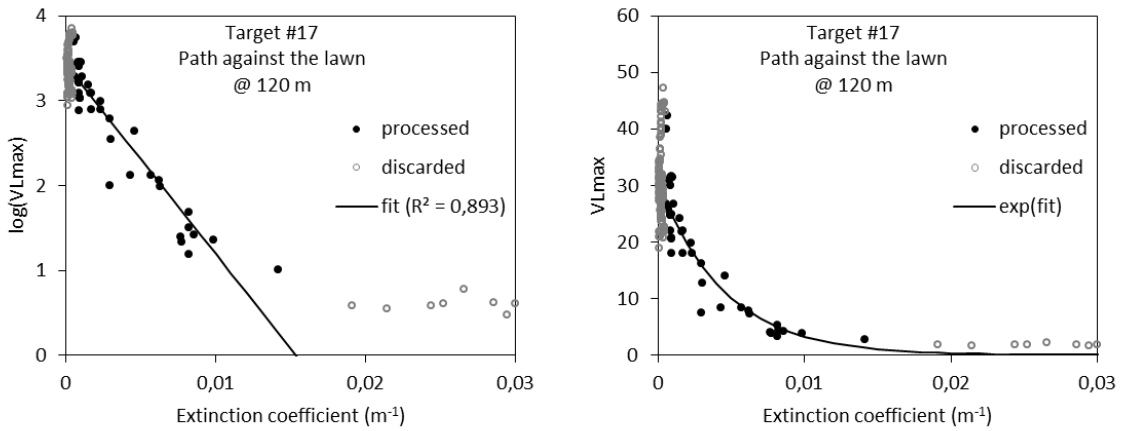

Figure 7 – Linear fit of log(TV) as a function of the extinction coefficient for target #17.

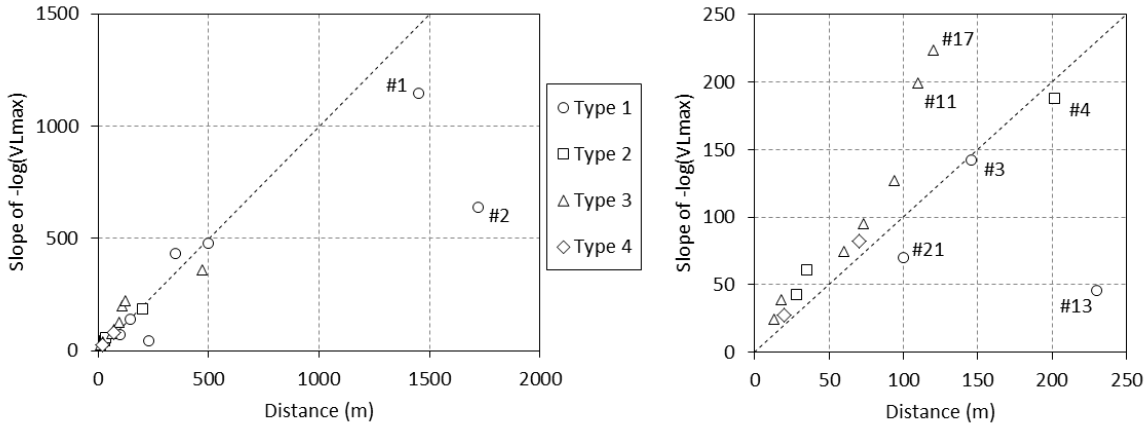

Figure 8 – Slope of the linear fit between log(TV) and the extinction coefficient, as a function of target distance, with different symbols for the different types of contrast, and a focus on distances under 250 m.

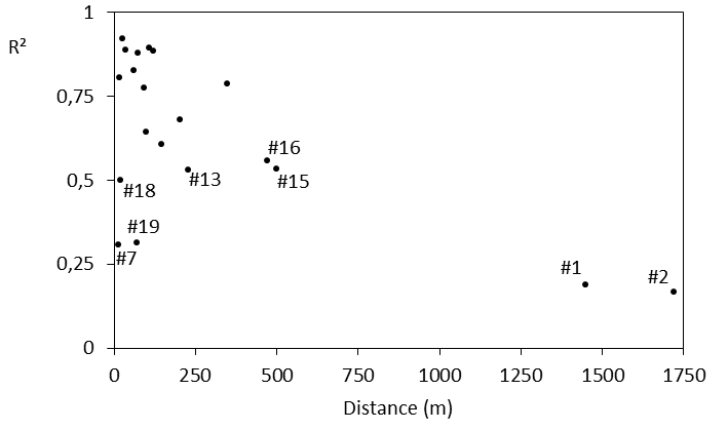

Figure 9 – R² values of the linear fit between log(TV) and the extinction coefficient, as a function of target distance.

There are some targets, however, for which the results do not concur with the hypothesis, as can be seen from the values of the coefficient of determination of the linear fit in Figure 9. This was expected for target #20 (R^2 = 0,012), a region in the sky with no particular feature except in good visibility conditions with partial cloud cover. As for targets #1 and #2 (the water towers, beyond 1 km), there are too few data left after applying the thresholds on MOR and VL for the results to be significant, because they are quite far from the camera. The same goes, to a lesser degree, for targets #15 (trees at 500 m) and #16 (building at 450 m): their visibility level drops below noise level sooner than closer targets as MOR decreases, leaving less data for the linear fit.

Targets #7 (feature on the roof) and #18 (lawn), on the contrary, are so close to the camera that fog has little effect on their visibility. Target #19 (lawn) also gets a low R^2 value: its VL values seldom exceed noise level, arguably because its spatial frequencies are too high for the camera, which renders the distant lawn as a smooth surface. R^2 values are higher than 0,5 for all the other targets.

The slope for target #13 (trees on the left) is only a fifth of the value predicted by the hypothesis: we believe this is caused by its proximity to the black border which is generated by the digital recorder in all images, like the timestamp (cf. Figure 1). The image processing approach implemented to compute the VL map works at several scales, so the low frequencies of this strong vertical contrast influence the visibility of neighbouring elements, independently of weather conditions. This dampens the influence of MOR on the visibility of

target #13. The same goes, to a lesser degree because it is closer to the camera, for target #21 (building on the right).

We also observe in Figure 8 that the slope value is above the diagonal for the majority of targets. This is consistent with our setting the distance of the targets as the minimum depth value when they actually involved a range of distance. It may at least partially explain the relatively large difference between the slope and the distance for targets #11 and #17, compared to targets #3 and #4 for which the distance was easier to estimate.

5 Conclusion

Using outdoor CCTV images and MOR measurements collected on a weather observation site, we investigated the relation between optical and computer vision estimates of visibility in daytime fog. We considered targets at different distances and with different types of contrast: objects against the sky, objects against a distant background, contrast between adjacent surfaces, and textures. We found a linear relationship between the natural logarithm of the visibility level v estimated from the images and the extinction coefficient k measured by the visibility sensor. We also found that the slope of the linear fit broadly corresponded with the distance d from the camera:

$$\log v \approx -kd + i \tag{2}$$

where i is the intercept of the linear fit. Equation (2) is equivalent to:

$$v \approx v_0 \exp(-kd) \tag{3}$$

where v_0 would be the value of VL in theoretical weather conditions, with diffuse lighting like in fog, but with a perfectly clear atmosphere. This value could find a use in the evaluation of defogging techniques (Tarel et al., 2012), since it provides a criterion to pick a reasonable reference for the restoration among images without fog in which contrasts, as we already pointed out, are very much dependent on lighting conditions.

Therefore, we bring empirical evidence indicating that Koschmieder's law applies not only to dark objects against the sky, but also to all kinds of non-luminous targets, even when they are not homogeneous in luminance or distance (at least up to a few hundred meters). However, we need to process more data before we can draw a general conclusion. We also demonstrate the benefit of computer vision for assessing contrast visibility in complex real-world scenes.

These findings are particularly interesting in the context of road traffic, as they contribute to a better understanding of the impact of daytime fog on the visibility of helpful (signs, markings) or hazardous (obstacles) elements in the field of view of the drivers. The potential applications lie mainly in the design of camera-based advanced driving aiding systems as well as adaptive road and vehicle speed advisory and lighting systems.

In future work, we intend to pursue the study with data from other observation sites. We will also work with synthetic images where the exact values of distance and intrinsic luminance will be known for all considered targets. This will help eliminate the ambiguity introduced into our analyses by the uncertainty about the depth values. It will also make it possible to further investigate the compatibility of visibility levels with Koschmieder's law.

References

ADRIAN, W. 1989. Visibility of Targets: Model for Calculation. *Lighting Research and Technology*, 21, 181-188.

AL-GHAMDI, A.S. 2007. Experimental Evaluation of Fog Warning System. *Accident Analysis and Prevention*, 39, 1065-1072.

BARTEN, P.G.J. 1999. *Contrast Sensitivity of the Human Eye and its Effects on Image Quality*. Bellingham: SPIE.

BRÉMOND, R. & BODARD, V. & DUMONT, E. & NOUAILLES-MAYEUR, A. 2013. Target Visibility Level and Detection Distance on a Driving Simulator. *Lighting Research and Technology*, 45 (1), 76-89.

CIE 1987. CIE 017.4-1987. *International Lighting Vocabulary*. Vienna: CIE.

CIE 1992. CIE 095-1992. *Contrast and Visibility*. Vienna: CIE.

COLOMB, M. & MORANGE, P. 2006. Visibility of Targets in Fog Conditions with Car Headlights. *Perception*, 35 (ECVP Abstract Supplement), 56.

HAUTIÈRE, N. & DUMONT, E. 2007. Assessment of Visibility in Complex Road Scenes Using Digital Imaging. CIE 178:2007. Proceedings of the 26th Session of the CIE, 4-11 July 2007, Beijing, China, D4, 96-99.

HAUTIÈRE, N. & BABARI, R. & DUMONT, E. & BRÉMOND, R. & PAPARODITIS, N. 2011. Estimating Meteorological Visibility using Cameras: A Probabilistic Model-Driven Approach. Computer Vision – ACCV 2010, *Lecture Notes in Computer Science*, 6495, 243-254.

JOULAN, K. & HAUTIÈRE, N. & BRÉMOND, R. 2011a. A Unified CSF-based Framework for Edge Detection and Edge Visibility. Proceedings of IEEE Conference on Computer Vision and Pattern Recognition Workshops, 20-25 June 2011, Colorado Springs, USA, 21-26.

JOULAN, K. & HAUTIÈRE, N. & BRÉMOND, R. 2011b. Contrast Sensitivity Function for Road Visibility Estimation on Digital Images. CIE 197:2011. Proceedings of the 27th Session of the CIE, 9-16 July 2011, Sun City, South Africa, 2(1), 1144-1149.

JOULAN, K. & HAUTIÈRE, N. & BRÉMOND, R. & ROBERT-LANDRY, C. 2014. Method for Determining the Visibility of Objects in the Field of View of the Driver of a Vehicle, taking into account a Contrast Sensitivity Function, Driver Assistance System and Motor Vehicle. European Patents 2747026 and 2747027, European Patent office.

TAREL, J.-P. & HAUTIERE, N. & CARAFFA, L. & CORD, A. & HALMAOUI, H. & GRUYER, D. 2012. Vision Enhancement in Homogeneous and Heterogeneous Fog. *IEEE Intelligent Transportation Systems Magazine*, 4(2):6-20.

WMO 2012. WMO-No. 8, 2nd ed. *Guide to Meteorological Instruments and Methods of Observation*. Geneva: WMO.